

Different regimes in vertical capillary filling

Siddhartha Das and Sushanta K. Mitra*

Micro & Nano-scale Transport Laboratory, Department of Mechanical Engineering, University of Alberta, Edmonton, Alberta, Canada T6G 2G8

(Received 30 September 2012; revised manuscript received 17 May 2013; published 12 June 2013)

In this paper, we identify that the different regimes encountered in a vertical capillary filling or a capillary-rise problem are determined entirely by two dimensionless parameters: Ohnesorge number (Oh) and Bond number (Bo). The initial universal inertial regime, which has been analyzed in our recent paper [Das *et al.*, *Phys. Rev. E* **86**, 067301 (2012)], is followed by any one of three possible regimes, dictated by the ratio Oh/Bo. For Oh/Bo \gg 1, the viscous effects dominate the gravitational effects, and one encounters the classical Washburn regime. For the other limit, i.e., Oh/Bo \ll 1, the viscous effects are insignificant and there is no Washburn regime. On the contrary, the inertial regime transits to the oscillatory regime with the filling length ℓ oscillating about the Jurin height ($\sim 1/\text{Bo}$), which is the maximum height attained by a liquid column in vertical capillary filling, with the viscous effects ($\sim \text{Oh}$) dictating the nature of the oscillations. For Oh/Bo \sim 1, we get a behavior intermediate of these two extreme regimes. Finally, we identify the correct force picture that drives the oscillatory regime and in the process achieve quantitative match with the experimental results, that was precluded in the previous studies.

DOI: 10.1103/PhysRevE.87.063005

PACS number(s): 47.55.nb

I. INTRODUCTION

For close to a century, studies of capillary rise in a vertical capillary have been one of the most well-addressed problems of capillarity [1–3]. The most well-appreciated understanding of the capillary-rise problem is the occurrence of the flow due to a balance of the capillary and the viscous forces and, therefore, a major volume of literature on capillary rise have mostly concentrated on demonstrating the occurrence of this regime, celebrated as the Washburn regime and characterized by $\ell \sim t^{1/2}$ (where ℓ is the filling length and t is the filling time) [1–3]. In fact, the capillary-rise problem has been shown to occur in a variety of different systems, e.g., in porous media [4–8], in multiphase system [9,10], in geometries of arbitrary shapes [11,12], in microgravity environment [13], etc., and in virtually all of them prevalence of the Washburn regimes has been identified as the overwhelming signature of capillary-rise phenomenon. Only relatively recently have researchers started to look beyond the Washburn regime in the context of capillary-rise phenomenon. The first important revelation has been the existence of an inertial regime, where the filling length ℓ remains small enough making the viscous effects negligible, and the flow occurs by a balance of the surface tension and the inertial effects [14]. This regime, where $\ell \sim t$, inevitably precedes the Washburn regime and occurs at early stages of capillary rise, i.e., for time $t \leq \tau_c$ (where τ_c is the capillary time scale [14]). The second major revelation has been identification of the cases where the effect of gravity overwhelms the viscous effect. Classically, the effect of gravity has only been considered implicitly in the description of the capillary problem. However, in these problems, typically valid for low viscosity liquids, the filling length oscillates about the Jurin height ℓ_J (Jurin height is the maximum height attained by the liquid column by a balance between the capillary and gravitational forces) [14]. This oscillatory regime, which now replaces the Washburn regime, is observed immediately after the initial inertial regime. In this paper, our focus is

to first understand the factors that dictate which one of the two regimes, Washburn or oscillatory, will follow the initial regime and then pinpoint the role of the different factors (e.g., viscosity, gravity, etc.) in the dynamics of these different regimes. In this context, it is important to pose our problem in the light of the current state of the art on these issues.

As discussed above, the understanding of the existence of the inertial regime has been rather recent. One of the pioneering studies in this context was by Quere [14], who experimentally demonstrated the existence of this inertial regime at the early stages of the capillary-rise problem. He found that in this regime $\ell \sim t$. This regime has been observed in several following investigations: in fact, this regime has been shown to be universally present in capillary filling problems for a plethora of capillary dimensions, varying from mm to nm [15,16]. In our recent paper [17], apart from establishing such universality of this regime through quantifications from existing literature, we also demonstrated that this regime will occur only when the filling length is small enough to ensure $(\ell/R)\text{Oh} \ll 1$ (where Oh is the Ohnesorge number and R is the capillary radius). The second major advancement of capillary-rise problems, beyond the understanding of the Washburn regime, has been the identification of the presence of an oscillatory regime, completely replacing the celebrated Washburn regime. This regime, just like the Washburn regime, follows the inertial regime. It primarily occurs for small viscosity liquids, and is characterized by the oscillation of the filling length about the Jurin height. Therefore, we no longer witness $\ell \sim t^{1/2}$, which is a signature of the Washburn regime; rather the filling length oscillates and, depending on the strength of the viscous effects, gradually damp out and equilibrates at the Jurin height. Like the identification of the inertial regime, for this problem, too, Quere [14] pioneered the experimental study, which demonstrated the existence of this oscillatory regime. Several subsequent studies confirmed the presence of this regime [18–20].

There are two major issues concerning this oscillatory regime that remain unaddressed, and the motivation of the present paper is to throw more light on these two issues.

*sushanta.mitra@ualberta.ca

First, what are the relevant physical parameters and conditions that dictate which one of the two regimes, Washburn or oscillatory, will follow the initial inertial regime? Second, what are the exact forces that are in action during this oscillatory regime? Regarding the first issue, to the best of our knowledge, there has been no definite identification of this relevant parameter space. This in a way is rather baffling, given that Quere [14] had already pointed out a quantification of the viscosity, for a given tube radius, for the appearance of the oscillatory regime. The closest study in this regard was by Fries and Dreyer [19], who, through a scaling analysis, identified several relevant dimensionless parameters for the capillary-rise problem; however, they failed to pinpoint the relevant parameter space for which the oscillatory regime replaces the Washburn regime. There is another related point regarding the transition from the inertial to oscillatory or Washburn regime. In our recent paper [17], we conclusively established that for cases where the inertial regime transits to the Washburn regime, the transition occurs when $(\ell/R)\text{Oh} \sim 1$. However, for the case where the inertial regime transits to the oscillatory regime, there exists no specification on the parameter space on when this transition will occur. The second issue, or the issue of the correct force picture during the oscillatory regime, is more involved, particularly stemming from the fact that a large number of models have been less successful in reproducing the exact experimental behavior, pointing towards an incomplete understanding of the correct force picture. One of the earlier attempts in this context was by Quere and Raphaël [21], who tried to analyze the oscillatory regime, but failed to reproduce the experimental observations. Zhmud *et al.* [18] suffered with similar failure. A more convincing attempt was made by Lorenceau *et al.* [22], who derived the governing equations (for the filling process, including the oscillatory regime) from the energy argument, and found a better match to the experimental results. Although this match is the closest possible representation of the experimental results, it fails to capture several key issues of the oscillatory regime, in particular the highly damped regime. For example, for a thick tube ($R = 1$ cm), the match can neither capture the amplitude nor the locations of the maxima and minima of the oscillations obtained from the experiments, whereas for a thinner tube ($R = 5$ mm) the mismatch is in capturing the locations of the maxima and minima of the oscillations. Both these issues stem from incorrect accounting of the retarding viscous effects and the driving capillary effects. In a recent paper, Masoodi *et al.* [23] attempts an energy-based analysis exactly similar to Lorenceau *et al.* [22], thereby suffering from the same gross limitations in the context of reproducing the experimentally observed oscillatory regime.

The above-described state of the art on the capillary-rise problem leads us to believe that the capillary-rise problem is yet to be fully understood due to lack of proper answers to several questions. We can summarize these questions as follows. What are the important physical parameters that dictate which one of two regimes, Washburn or oscillatory, will follow the inertial regime? Given that the inertial regime will transit to the oscillatory regime, what physical parameters dictate the occurrence of this transition? What is the role of viscosity in the oscillatory regime? Can we correctly identify the forces at play during the oscillatory regime,

so that we can ensure that, unlike the existing studies, numerical and theoretical calculations can actually reproduce the experimentally observed [14] oscillatory regime? etc.

In this paper, through scaling analysis and analytical and numerical solutions, we establish that the entire capillary-rise problem is dictated by two dimensionless physical parameters: Ohnesorge number (Oh) and Bond number (Bo). Following the initial inertial regime [14,17], one can witness any one of three regimes: for $\text{Oh}/\text{Bo} \gg 1$ the viscous effects are important, ensuring that the inertial regime transits to Washburn regime, for $\text{Oh}/\text{Bo} \ll 1$, the gravitational effect dominates the viscous retardation so that the inertial regime transits to the oscillatory regime with the filling length oscillating about the Jurin height ℓ_J (where $\ell_J \sim 1/\text{Bo}$), and, finally, for $\text{Oh}/\text{Bo} \sim 1$, we get a behavior intermediary to these two extreme cases. Therefore, we establish that the Oh/Bo ratio dictates which one of the two, Washburn or oscillatory regimes, will follow the inertial regime. We also define an equivalent critical radius, which, analogous to the Oh/Bo ratio, acts as a factor that dictates this transition. Secondly, given that the inertial regime will transit to the oscillatory regime, we identify the condition on when this will occur. When the inertial regime transits to the Washburn regime, this transition has been shown to occur when $(\ell/R)\text{Oh} \sim 1$ [17]. On the contrary, we show that when the inertial regime transits to the oscillatory regime, this transition will happen for $(\ell/R)\text{Oh} \ll 1$. Therefore, in the present paper we identify parameter spaces for two different events. First, we identify the parameter space which dictates which one of the two regimes, oscillatory or Washburn, will follow inertial regime and, second, we identify, given that the inertial regime will transit to the oscillatory regime, the relevant parameter space for this transition. Third, we pinpoint the role of viscosity ($\sim \text{Oh}$) in dictating the oscillatory regime: we highlight the nontrivial aspect of this dependence, given the fact that the oscillatory regime appears only when the viscous effects are dominated by the gravity forces. Finally, we provide extensive comparisons of our model with the experimental results of capillary rise for different liquids in capillaries of varying dimensions. First, we compare our model with the experimental results of Quere [14], and find excellent match for both the cases of low viscosity (case of oscillatory regime) and high viscosity (case of Washburn regime) liquids. We demonstrate that to achieve such a close match, we need to use fitting parameters to describe the driving surface-tension force and the retarding drag force. We subsequently establish that use of such fitting constants leads to a prediction of the experimental results (e.g., results of capillary rise of diethyl ether in thinner capillaries [18]) that is substantially more improved than that obtained with the existing model [18]. In fact, in the process of faithfully reproducing the experimental results, we identify the correct forces that are in action during the post-inertial regime (Washburn or oscillatory) of the capillary filling process.

Before starting the analysis, it is important to pinpoint the key differences of this paper with our recent paper on capillary filling [17]. Our recent paper [17] concentrated solely on analyzing the inertial regime. In that paper, we identified the time scale and the physical parameters that dictated the occurrence and prevalence of this regime, and the transition of this regime to the Washburn regime. Therefore, this paper

virtually never looked beyond the inertial regime. On the contrary, the main focus of the present paper is to look beyond this inertial regime and analyze in detail the two possible regimes, Washburn or oscillatory, that will follow the inertial regime. Therefore, the present paper is completely different in scope as compared to our previous paper: it can be argued that both these papers address the broad problem of capillary filling; however, they highlight two completely segregated aspects of the problem.

II. SCALING ESTIMATES

In our previous paper [17], we have demonstrated that a capillary filling problem, irrespective of whether it is a problem of horizontal or vertical capillary filling, is universally characterized by an initial inertial regime (where $\ell \sim t$ [14]), and obtained the physical conditions that dictate the occurrence of this regime. In vertical capillaries, in the regime following this inertial regime, the capillary drive will be retarded by a combination of the gravitational (F_g) and the viscous forces (F_v). The ratio of these two retarding forces can be expressed as, with the characteristic velocity $u_0 \sim \ell/t$ and the characteristic transverse dimension $y \sim R$,

$$\frac{F_v}{F_g} \sim \frac{\eta(du/dy)R\ell}{R^2\ell\rho g} \sim \frac{\eta u_0\ell}{\rho g R^2\ell} \sim \frac{\eta\ell}{\rho g R^2 t}, \quad (1)$$

where η is the dynamic viscosity of the liquid and g is the acceleration due to gravity. The flow being always driven by the capillary forces, we may write $\frac{d}{dt}(\rho\ell R^2 u_0) \sim \gamma R \Rightarrow t \sim (\frac{\rho\ell^2 R}{\gamma})^{1/2}$ [17], so that Eq. (1) reduces to

$$\frac{F_v}{F_g} \sim \frac{\eta}{(\rho R \gamma)^{1/2}} \frac{\gamma}{\rho g R^2} \sim \frac{\text{Oh}}{\text{Bo}}, \quad (2)$$

where $\text{Oh} = \eta/(\rho R \gamma)^{1/2}$ is the Ohnesorge number and $\text{Bo} = \rho g R^2/\gamma$ is the Bond number. Therefore, during capillary rise, following the inertial regime, we can have three different types of regimes based on the variation of the Oh/Bo ratio. In fact, we can identify these three regimes, alternatively, by defining a critical radius (obtained from the condition when $\text{Oh} \sim \text{Bo}$):

$$R_c = \left(\frac{\eta^2 \gamma}{\rho^3 g^2} \right)^{1/5}. \quad (3)$$

These three regimes can be defined as follows.

(1) For $\text{Oh}/\text{Bo} \gg 1$ or $R \ll R_c$, the impact of the gravity is negligible (except at the very end of the filling), and we have the perfect Washburn regime (see later) following the inertial regime.

(2) For $\text{Oh}/\text{Bo} \ll 1$ or $R \gg R_c$, the impact of viscous force is negligible, and we do not encounter any Washburn regime at all; rather the inertial regime transits to the oscillatory regime where ℓ oscillates (before equilibrating at ℓ_J) about ℓ_J (see later).

(3) For $\text{Oh}/\text{Bo} \sim 1$ or $R \sim R_c$, the two effects balance each other and, following the inertial regime, we encounter the behavior intermediate to the Washburn and the oscillatory regimes.

III. ANALYTICS FOR THE GRAVITY-DOMINATED CASE

The net force balance can be expressed as

$$\frac{d}{dt} \left[\pi \rho R^2 \ell \frac{d\ell}{dt} \right] = K_1 \frac{2\gamma \cos \theta}{R} (\pi R^2) - \pi \rho R^2 \ell g. \quad (4)$$

In (4), θ is the dynamic contact angle, and the factor K_1 represents the contribution of the possible nontrivial effects, e.g., formation of precursor film [24], capillary wall roughness [25], etc., that may affect the capillary drive. Equation (4) can be expressed in dimensionless form as $\frac{d}{d\bar{t}}(\bar{\ell} \frac{d\bar{\ell}}{d\bar{t}}) \approx A - B\bar{\ell}$, where $\bar{\ell} = \ell/R$, $\bar{t} = t/\tau_c$, $A = 2K_1\gamma \cos \theta \tau_c^2/\rho R^3 = 2K_1 \cos \theta$ and $B = g\tau_c^2/R = \rho g R^2/\gamma = \text{Bo}$. Integrating this equation twice under the condition that the solution passes through zero and $\bar{\ell}_{\bar{t}=0} = 0$, we get

$$\bar{\ell} = A^{1/2} \bar{t} - \frac{B}{6} \bar{t}^2. \quad (5)$$

Equation (5) reduces to the form obtained by Quere [14] with $A = B = 1$. The condition when the flow will stop, i.e., $d\bar{\ell}/d\bar{t} = 0$, yields $\bar{t} = \frac{3A^{1/2}}{2B} = \frac{3(2K_1 \cos \theta)^{1/2}}{\text{Bo}} \Rightarrow (\ell/R)\text{Oh} = 3(2K_1 \cos \theta)^{1/2}(\text{Oh}/\text{Bo})$. Therefore, for $\text{Oh}/\text{Bo} \ll 1$, i.e., the condition when the gravitational effects dominate the viscous retardation effects, the flow will stop (or the filling length attains the Jurin height, and oscillates about the Jurin height) for $(\ell/R)\text{Oh} \ll 1$. In other words, this signifies that the inertial regime (where $\ell \sim t$) transits to the oscillatory regime (signature of the $\text{Oh}/\text{Bo} \ll 1$ case) for $(\ell/R)\text{Oh} \ll 1$. This is a completely different finding in the light of the fact that in our recent paper [17] we identified that the inertial regime transits to the Washburn regime for $(\ell/R)\text{Oh} \sim 1$.

IV. ANALYTICS FOR THE VISCOSITY DOMINATED CASE

The governing equation can be expressed in dimensional form as

$$\frac{d}{dt} \left[\pi \rho R^2 \ell \frac{d\ell}{dt} \right] = K_1 \frac{2\gamma \cos \theta}{R} (\pi R^2) - K_2 \pi \eta \ell \frac{d\ell}{dt}. \quad (6)$$

In (6) K_2 represents the effect of possible deviation (from the fully developed parabolic profiles) of the velocity profiles at different depths (inside the liquid column) from the liquid-air interface. The viscous drag being computed using the velocity gradient at the capillary wall, this implies that $K_2 \neq 8$ ($K_2 = 8$ for fully developed velocity profiles [19]). Equation (6) can be expressed in dimensionless form as $\frac{d}{d\bar{t}}(\bar{\ell} \frac{d\bar{\ell}}{d\bar{t}}) = A - C\bar{\ell} \frac{d\bar{\ell}}{d\bar{t}}$, where $C = K_2 \eta \tau_c / \rho R^2 = K_2 \tau_c / \tau_v = K_2(\text{Oh})$ (here $\tau_v = \rho R^2/\eta$ is the viscous time scale). We integrate the above equation twice (in the presence of the condition $d\bar{\ell}/d\bar{t} = 0$, $\bar{\ell} = 0$ at $\bar{t} = 0$) to obtain

$$\bar{\ell}^2 = 2 \frac{A\bar{t}}{C} - \frac{2A}{C^2} [1 - \exp(-C\bar{t})]. \quad (7)$$

Expressions analogous to (7) have been obtained by other authors [3,20]. Please note that for very small t or \bar{t} , we can simplify (7) as $\bar{\ell}^2 \approx 2 \frac{A\bar{t}}{C} - \frac{2A}{C^2} [1 - 1 + C\bar{t} - C^2\bar{t}^2/2] \Rightarrow \bar{\ell} \approx A^{1/2} \bar{t} \Rightarrow \ell \sim t(\gamma/\rho R)^{1/2}$ [17]. For larger time, i.e., $\tau_c < t < \tau_v$, we can obtain [by using $\exp(-C\bar{t}) \approx \exp(-K_2 t/\tau_v) \approx 1]$ $\bar{\ell} = (2A/C)^{1/2} (\bar{t})^{1/2} \Rightarrow \ell \sim (\gamma R/\eta)^{1/2} t^{1/2}$, i.e., we recover the Washburn regime [2,17].

V. NUMERICAL SOLUTION

The governing equation with all the terms can be expressed (in dimensionless form) as

$$\frac{d}{d\bar{t}} \left(\bar{\ell} \frac{d\bar{\ell}}{d\bar{t}} \right) = A - C\bar{\ell} \frac{d\bar{\ell}}{d\bar{t}} - B\bar{\ell}. \quad (8)$$

We solve (8) numerically in the presence of the conditions $(\bar{\ell})_{\bar{t}=0} = (d\bar{\ell}/d\bar{t})_{\bar{t}=0} = 0$.

VI. RESULTS AND DISCUSSIONS

Figure 1 shows the analytical and numerical results for the $\bar{\ell}$ versus \bar{t} variation for $C/B = K_2(\text{Oh}/\text{Bo}) \gg 1$ (i.e., cases where the viscous effects dominate the gravitational effects). Therefore, such cases are effectively analogous to horizontal capillary filling (except at the very end of the filling time, when gravitational effects take over). In fact, this demarcation can be witnessed by comparing the numerical and the analytical results: for lesser time (when the effect of gravity is negligible), one finds excellent match between the numerical and the analytical results; but at instants close to when the filling stops, the effect of gravity becomes important, thereby showing a saturation in the numerical results (which consider gravity), whereas the analytical results (without the effect of gravity) shows no saturation. Plots in Fig. 1 exhibit the attainment of a distinct viscosity-governed Washburn regime, indicating the impact of $\text{Oh}/\text{Bo} \gg 1$. Figure 1 clearly shows that the transition between the linear and the Washburn regimes occurs when $(\bar{\ell})\text{Oh} = (\ell/R)\text{Oh} \sim 1$, as has been suggested previously [17]: for smaller C/B ratio, therefore, the transition is triggered at a larger ℓ/R . Figure 1 also demonstrates the impact of the capillary drive, manifested by the quantity A . Smaller A implies lesser drive, implying a greater inertial effect manifested through the occurrence of transition between the linear and the Washburn regimes at a larger ℓ/R .

Figure 2 shows the $\bar{\ell}$ versus \bar{t} variation for the gravity-dominated cases [i.e., when $C/B = K_2(\text{Oh}/\text{Bo}) \ll 1$]. Like the case of the other extreme ($C/B \gg 1$), here too one witnesses the *linear* regime for small \bar{t} , and for this regime there is an excellent match between the numerical and the analytical results. In fact, similar to the model by Quere [14],

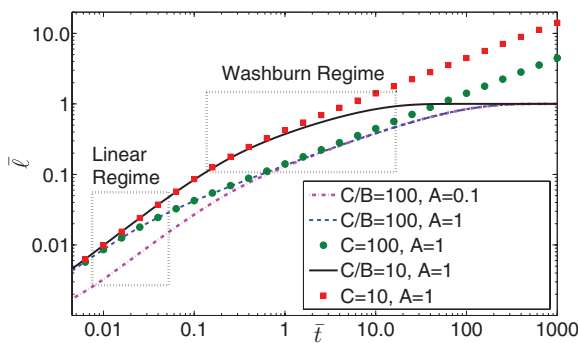


FIG. 1. (Color online) Analytical and numerical results for the $\bar{\ell}$ versus \bar{t} variation for $C/B = K_2(\text{Oh}/\text{Bo}) \gg 1$ and $A/B = 1$. Results from analytical and numerical calculations are shown by markers and continuous lines, respectively. We also indicate the linear and the Washburn regimes.

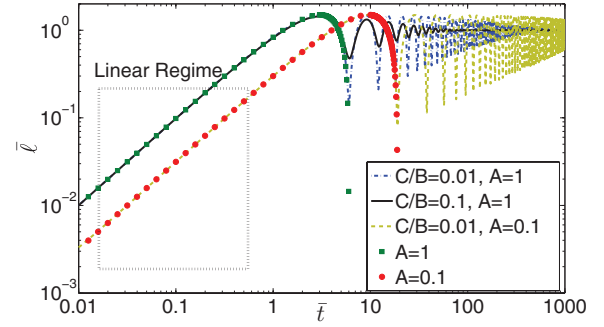


FIG. 2. (Color online) Analytical and numerical results for the $\bar{\ell}$ versus \bar{t} variation for $C/B = K_2(\text{Oh}/\text{Bo}) \ll 1$ and $A/B = 1$. Results from analytical and numerical calculations are shown by markers and continuous lines, respectively. We also indicate the linear regime.

analytical results show a perfect match for the linear regime and the first part of the rise, but fail to reproduce the subsequent oscillations of the numerical results. Figure 2 clearly shows that for this case the linear regime transits to the oscillatory regime for $(\bar{\ell})\text{Oh} \ll 1$ [here $C = K_2(\text{Oh})$ gives a measure of the Ohnesorge number], as has been illustrated in Sec. III. This is in distinct contrast to the transition from the inertial to the Washburn regime, which occurs for $(\ell/R)\text{Oh} \sim 1$ (see [17] and previous paragraph). The most important observation of Fig. 2 is that, due to the insignificant contribution of the viscous drag, there is no Washburn regime, following the inertial regime and the inertial regime directly transits to the oscillatory regime with oscillations (of $\bar{\ell}$) about the Jurin height $[\bar{\ell}_J = A/B = 2\gamma \cos \theta / \rho g R^2 \sim 1/\text{Bo}$ (with $K_1 = 1$)]. The net force on the rising liquid column is $A - B\bar{\ell} = A(1 - \bar{\ell}/\bar{\ell}_J)$. Hence one gets the oscillations about $\bar{\ell}_J$. Therefore, when the capillary drive is weak (i.e., A is small), Jurin height is attained at a later time, triggering the oscillations at a later time. Lower viscosity [or smaller $C = K_2(\text{Oh})$] leads to lesser damping and higher amplitude of the oscillations. This is rather nontrivial: the insignificant influence of the viscous forces ensures that there is no Washburn regime and the inertial regime transits to the oscillatory regime, but the oscillations themselves are controlled by the viscosity. The fact that there are oscillations and the filling length can attain any finite height (Jurin height, although Jurin height is independent of viscosity) at equilibrium, occurs solely due to the presence of a viscous liquid: in the case of a perfectly inviscid liquid, the liquid column will rise and fall back to the reservoir (equivalent to the case of a stone moving up and coming down in air), without causing any finite capillary rise.

Figure 3 shows the $\bar{\ell}$ versus \bar{t} variation for $C/B = K_2(\text{Oh}/\text{Bo}) \sim 1$. Other than the universal linear regime present in all the plots, one can clearly witness the gradual transition from the oscillatory to the nonlinear (with slope less than 1), nonoscillatory regime with an increase in the C/B ratio. Smaller A or weaker drive ensures a larger oscillation (also witnessed in Fig. 2) for a given C/B . Figures 1–3 provide answers to three key questions put forward in the first part of the paper. First, it clearly shows that ratio Oh/Bo , proportional to the ratio C/B , dictates which one of the two regimes, Washburn or oscillatory, will follow the inertial regime in a capillary-rise problem. Second, it is established

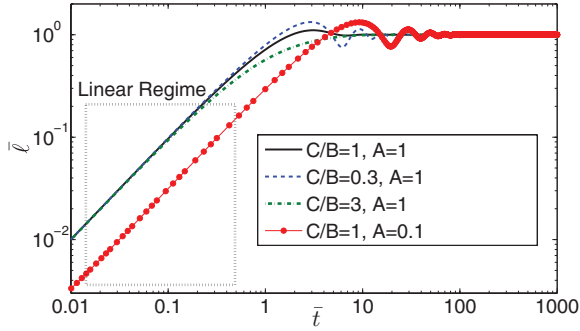


FIG. 3. (Color online) Numerical results for the ℓ versus t variation for $C/B = K_2(\text{Oh}/\text{Bo}) \sim 1$. We also indicate the linear regime. For all the plots we take $A/B = 1$.

that if the inertial regime transits to the oscillatory regime, then the transition occurs for $(\ell/R)\text{Oh} \ll 1$. Third, the impact of the viscosity in the nature of the oscillations are explicated: the nontriviality of the scenario, on account of the fact that the oscillations appear only when the gravity effects dominate viscous retardations, are clearly highlighted in a manner that has been missing from similar previous studies [19].

Figure 4 compares our numerical model with the experimental results of Quere [14] for two different liquids (ether and ethanol) having large differences in viscosity (which thereby provides disparate ranges of Oh/Bo values). In the numerical results, K_1 and K_2 are used as fits. We find $K_2 = 15$ (i.e., $\neq 8$) for both ether and ethanol, whereas $K_1 \cos \theta = 0.95$ for ether and $K_1 \cos \theta = 0.5$ for ethanol. We shall discuss the significance of these fitting parameters later. To provide a more substantiative demonstration of the validity of our proposed model, we further compare our numerical model

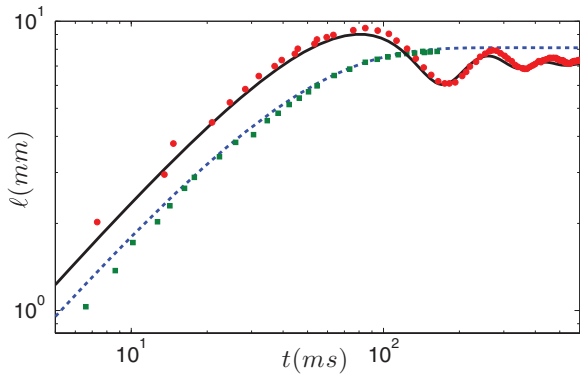


FIG. 4. (Color online) Comparison with the experimental results of Quere [14] on capillary rise (capillary radius $R = 689 \mu\text{m}$) for ether (shown in red circles; corresponding properties are $\rho = 710 \text{ kg/m}^3$, $\gamma = 16.6 \text{ mN/m}$, $\eta = 0.3 \text{ mPas}$, and $\ell_J = 7.1 \text{ mm}$; hence $\tau_c = 3.7 \text{ ms}$, $\text{Oh} = 0.0033$, $\text{Bo} = 0.1990$, and $\text{Oh}/\text{Bo} = 0.0167$) and ethanol (shown in green squares; corresponding properties are $\rho = 780 \text{ kg/m}^3$, $\gamma = 21.6 \text{ mN/m}$, $\eta = 1.17 \text{ mPas}$, and $\ell_J = 8.1 \text{ mm}$; hence $\tau_c = 3.4 \text{ ms}$, $\text{Oh} = 0.0109$, $\text{Bo} = 0.1680$, and $\text{Oh}/\text{Bo} = 0.0646$). Numerical results are shown by continuous lines: black bold line is used for the case of ether (corresponding fitting parameters are $K_1 \cos \theta = 0.95$ and $K_2 = 15$) and blue dashed line is used for the case of ethanol (corresponding fitting parameters are $K_1 \cos \theta = 0.5$ and $K_2 = 15$).

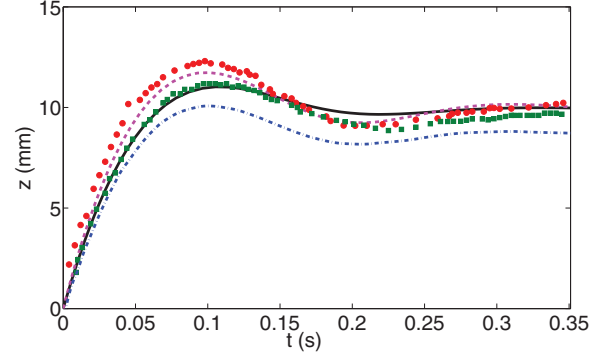


FIG. 5. (Color online) Comparison with the experimental results of Zhmud *et al.* [18] on capillary rise for diethyl ether in capillaries (of radius $R = 0.5 \text{ mm}$) with different lengths L . The experimental results are shown by markers (results corresponding to $L = 0.05 \text{ m}$ is shown in red circles and that corresponding to $L = 0.1 \text{ m}$ is shown in green squares) and the numerical results from our proposed model are shown by continuous lines (results corresponding to $L = 0.05 \text{ m}$ are shown in dashed magenta line and results corresponding to $L = 0.1 \text{ m}$ are shown in black bold line). The numerical results proposed by Zhmud *et al.* [18] for $L = 0.05 \text{ m}$ are shown in blue dash-dotted line. The properties used for the simulation are $\rho = 710 \text{ kg/m}^3$, $\gamma = 16.7 \text{ mN/m}$, $\eta = 0.22 \text{ mPas}$, and $\eta_g = 0.0186 \text{ mPas}$ (which yields $\ell_J = 9.9 \text{ mm}$, $\tau_c = 2.3 \text{ ms}$, $\text{Oh} = 0.0028$, $\text{Bo} = 0.1$, and $\text{Oh}/\text{Bo} = 0.028$). The fitting parameters used for the present numerical result are $K_1 \cos \theta = 1.0$ and $K_2 = 13$.

with the experimental results of filling of capillaries by diethyl ether [18]. The experiments had been performed for capillaries of different lengths, and we provide the comparison for those values of capillary lengths where the filling length exhibits oscillations. The key thing to note is that our governing equation for the capillary filling dynamics [Eq. (8)] does not account for the length dependence of the capillary. Following Zhmud *et al.* [18], such a dependence is introduced by considering an additional viscous drag force that results on account of the capillary liquid displacing another fluid (usually vapor or air) and can be expressed as $K_2 \pi \eta_g (L - \ell)(d\ell/dt)$ (where η_g is the viscosity of the displaced fluid and L is the capillary length). Typically, η_g being substantially small, only when the filling liquid has sufficiently low viscosity will this additional drag force contribution be important. Figure 5 clearly demonstrates that our numerical model leads to a substantially better prediction of the oscillation behavior, as compared to the prediction provided by Zhmud *et al.* [18], thereby establishing the need for using the fitting constants $K_1 \cos \theta$ and K_2 (in Fig. 5, we use $K_1 \cos \theta = 1$ and $K_2 = 13$) in the capillary-rise model.

A. Significance of the fitting constants

The most essential ingredient of our model is the use of the fitting parameters $K_1 \cos \theta$ and K_2 to respectively model the capillary drive and the viscous drag. Use of such fitting parameters has been absent in earlier models; however, as shown above, they are essential to provide a more acceptable match to the experimental results as compared to those obtained with existing numerical results. The first fitting parameter $K_1 \cos \theta$ dictates the driving capillary forces, and

therefore is directly related to issues such as the dynamic contact angle (since this θ is the dynamic contact angle), precursor film, etc. There is a plethora of literature that expresses the dynamic contact angle as a function of the capillary number ($Ca = U\eta/\gamma$, where U is the filling speed) [20,26,27] and the equilibrium contact angle θ_e . Therefore, even when θ_e becomes identical (often dictated by the corresponding surface tension), variation in η , which will vary Ca , may change the dynamic contact angle. For example, ethanol and ether (two fluids whose filling behavior are studied in Fig. 4) have identical surface-tension values, but disparate viscosities, thereby leading to substantial difference in the corresponding capillary numbers and hence $\cos\theta$. Using $\theta_e \approx 0$ for both the liquids, and $U = d\ell/dt \sim \sqrt{\gamma/\rho R}$ (considering the linear regime, for example), we get $(\cos\theta)_{\text{ethanol}} = 0.59$ and $(\cos\theta)_{\text{ether}} = 0.82$ [using $\cos\theta = \cos\theta_e - (1 + \cos\theta_e) \tanh(4.96Ca^{0.702})$ [27]] and $(\cos\theta)_{\text{ethanol}} = 0.58$ and $(\cos\theta)_{\text{ether}} = 0.77$ [using $\cos\theta = \cos\theta_e - 2(1 + \cos\theta_e)Ca^{0.5}$ [20]]. Therefore, we can clearly see that the cosine of the dynamic contact angle for ether is more than that of ethanol, and this justifies our choice of using larger $K_1 \cos\theta$ for ether as compared to ethanol. For the results corresponding to diethyl ether (see Fig. 5 and [18]) (with $\theta_e = 26^\circ$), we get $\cos\theta = 0.87$ [using $\cos\theta = \cos\theta_e - (1 + \cos\theta_e) \tanh(4.96Ca^{0.702})$ [27]] and $\cos\theta = 0.84$ [using $\cos\theta = \cos\theta_e - 2(1 + \cos\theta_e)Ca^{0.5}$ [20]]. From the closeness of values of $\cos\theta$ between the ether and diethyl ether, we can justify similar $K_1 \cos\theta$ values for the two cases. Please note the above analysis only provides an indication of the qualitative variation of the $K_1 \cos\theta$ values between different liquids—to obtain the exact values of $K_1 \cos\theta$ (which will match with the values used for fitting) we need to perform rigorous molecular scale simulations of the interactions between the filling liquids and the capillary walls, which is beyond the scope of the present study. The fit parameter $K_1 \cos\theta$ can be considered to reflect the effect of wetting of the capillary walls by the filling liquid. Therefore, issues such as presence of a precursor film (and the structure of the precursor film) [24,25], capillary wall roughness [25], etc., which have been previously pointed out to affect the capillary filling process, will also influence the parameter $K_1 \cos\theta$.

The second fitting parameter is K_2 , which dictates the drag force experienced by the filling liquid. The drag force being a function of the transverse velocity gradient at the capillary wall, one needs the exact velocity profile to calculate it. The classical approach has been to assume a fully developed Poiseuille flow field, which will yield $K_2 = 8$. However, the fit to the experimental results are obtained with much higher values of K_2 , namely $K_2 = 15$ for the experimental results of Quere (with capillary radius $R = 0.689$ mm) [14] (see Fig. 4) and $K_2 = 13$ for experimental results of Zhmud *et al.* (with capillary radius $R = 0.5$ mm) [18] (see Fig. 5). Deviation of K_2 values from the classical case of $K_2 = 8$ occurs due to the fact that the fully developed profile (which leads to $K_2 = 8$) will occur only substantially downstream of the liquid-air interface; at locations close to the liquid-air interface, the bulk remains unaffected, and therefore the velocity gradients at the wall (used to calculate the drag) would be steeper, leading to larger values of K_2 . Also different fitting values of K_2 for different capillary radii (see Figs. 4 and 5) can be explained by arguing that, for channels with smaller radii, there

is lesser distinction between “near-wall” and bulk regions of the capillary, and consequently the difference in K_2 values, caused by the steepness in the velocity gradients close to the wall (with the bulk remaining unaffected), will be less severe.

It is to be clearly noted that these two fitting parameters, $K_1 \cos\theta$ and K_2 , play distinctly different roles in reproducing the different regimes during the capillary filling process. $K_1 \cos\theta$ dictates the driving force for filling, and its variation and dependence on issues such as liquid viscosity can be at least qualitatively hypothesized from dependence of dynamic contact angles on capillary number, etc. On the contrary, use of a value of $K_2 \neq 8$ [i.e., calculation of drag (for capillary filling) considering velocity profiles other than the fully developed parabolic profiles] is very new in the context of the existing studies [14,19,21–23]. Nevertheless, use of both the fitting parameters are unavoidable to ensure acceptable match with the oscillatory behavior demonstrated in the experimental results. In Fig. 5, we pinpoint the relevance of these individual fitting parameters in faithfully reproducing the experimental behavior. In Fig. 5, we show the manner in which the numerical result of Zhmud *et al.* [18] deviates from the corresponding experimental results. In the numerical result of Zhmud *et al.* [18], a lesser value of the driving capillary force (caused by the absence of the appropriate fitting value of $K_1 \cos\theta$) ensures that the filling length (at all times) obtained from the numerical prediction is substantially lower than the experimental results, and the Jurin height about which the filling length oscillates is also lesser. Secondly, a weaker value of the viscous drag force (caused by the use of $K_2 = 8$) ensures that in the oscillatory regime the filling length oscillates more vigorously (i.e., with a larger amplitude and/or frequency) than that observed in the experiments (e.g., the numerical results show two maxima in a time span of 0.35 s, whereas the experimental results show only one). In our proposed numerical model, on the other hand, use of the appropriate fitting parameters ensure that we indeed get a much better reproduction of the experimental results. In fact, this comparison allows us to infer the possible effect in using $K_2 = 8$ in the numerical model in order to match the experimental results of Quere [14] (see Fig. 4)—for ether (whose viscosity is small enough to cause oscillations) the oscillations will be substantially more vigorous (with larger amplitude and/or frequency) than that observed in experiments, whereas for ethanol (whose viscosity is too large to cause oscillations and the filling length obeys the Washburn regime), oscillations may be triggered so that, completely contrary to the experimental results, the oscillatory regime will follow the inertial regime.

As a closing remark, it is useful to emphasize that the parameters $K_1 \cos\theta$ and K_2 still remain as fit parameters, and we have only provided a qualitative argument justifying their choices. Importantly, however, use of these fit parameters clearly bring out the lacuna of the existing understanding of the forces at work during the capillary filling process. This limitation is particularly manifested while reproducing the oscillatory regime, where correct accounting of the drag forces are needed. This motivates the use of $K_2 > 8$, establishing that the drag force in capillary filling should not be computed considering fully developed flow from the outset. However, this inference is constrained by the fact that it uses fitting parameters and justifies these parameters from a qualitative

argument. A more complete model is required, which would provide the correct “no-fitting-parameter” description of the drag forces by considering the necessary picture of the developing flow field in the capillary. We are in the process of developing such a model, and validate it through micro-Particle Image Velocimetry experimental results. Findings of that study will be presented in a future publication.

VII. CONCLUSIONS

We have identified that the different possible regimes in vertical capillary filling are dictated by two dimensionless physical parameters: Ohnesorge number (Oh) and the Bond number (Bo). For $Oh/Bo \gg 1$, the filling is dictated by a combination of linear and viscous (Washburn) regimes, whereas

for $Oh/Bo \ll 1$, the filling is dictated by a combination of linear and oscillatory regimes. For the latter case, the effect of gravity outweighs the viscous drag; but counterintuitively it is viscosity that dictates the nature of the oscillations and the attainment of an equilibrium height. In fact the correct description of the viscous retardation effects holds the key to perfectly describe the oscillatory regime, and obtain a satisfactory match with the experimental results of oscillations [14,18].

ACKNOWLEDGMENTS

The authors gratefully acknowledge the Natural Sciences and Engineering Research Council of Canada (NSERC) for providing financial support to S.D. in the form of the Banting Postdoctoral Fellowship.

-
- [1] R. Lucas, *Kolloid Z.* **23**, 15 (1918).
 [2] E. W. Washburn, *Phys. Rev.* **17**, 273 (1921).
 [3] C. H. Bosanquet, *Philos. Mag.* **45**, 525 (1923).
 [4] J. van Brakel and P. M. Heertjes, *Nature (London)* **254**, 585 (1975).
 [5] T. Delker, D. B. Pengra, and P. Z. Wong, *Phys. Rev. Lett.* **76**, 2902 (1996).
 [6] M. Lago and M. Araujo, *Physica A* **289**, 1 (2001).
 [7] A. Hamraoui and T. Nylander, *J. Colloid Interface Sci.* **250**, 415 (2002).
 [8] B. J. Mullins and R. D. Braddock, *Int. J. Heat Mass Transfer* **55**, 6222 (2012).
 [9] K. S. Sorbie, Y. Z. Wu, and S. R. McDougall, *J. Colloid Interface Sci.* **174**, 289 (1995).
 [10] F. Maggi, *Colloid Surf. A* **415**, 119 (2012).
 [11] D. Erickson, D. Li, and C. B. Park, *J. Colloid Interface Sci.* **250**, 422 (2002).
 [12] Z. Wang, C. C. Chang, S. J. Hong, Y. J. Sheng, and H. K. Tsao, *Langmuir* **28**, 16917 (2012).
 [13] M. Dreyer, A. Delgado, and H-J. Rath, *J. Colloid Interface Sci.* **163**, 158 (1994).
 [14] D. Quere, *Eur. Phys. Lett.* **39**, 533 (1997).
 [15] L. Joly, *J. Chem. Phys.* **135**, 214705 (2011).
 [16] S. Supple and N. Quirke, *Phys. Rev. Lett.* **90**, 214501 (2003).
 [17] S. Das, P. R. Waghmare, and S. K. Mitra, *Phys. Rev. E* **86**, 067301 (2012).
 [18] B. V. Zhmud, F. Tiberg, and K. Hallstenson, *J. Colloid Interface Sci.* **228**, 263 (2000).
 [19] N. Fries and M. Dreyer, *J. Colloid Interface Sci.* **338**, 514 (2009).
 [20] N. Fries and M. Dreyer, *J. Colloid Interface Sci.* **327**, 125 (2008).
 [21] D. Quere and E. Raphaël, *Langmuir* **15**, 3679 (1999).
 [22] E. Lorenceau, D. Quere, J-Y. Ollitrault, and C. Clanet, *Phys. Fluids* **14**, 1985 (2002).
 [23] R. Masoodi, E. Languri, and A. Ostadhossein, *J. Colloid Interface Sci.* **389**, 268 (2013).
 [24] S. Chibbaro, L. Biferale, F. Diotallevi, S. Succi, K. Binder, D. Dimitrov, A. Milchev, S. Girardo, and D. Pisignano, *Eur. Phys. Lett.* **84**, 44003 (2008).
 [25] S. Chibbaro, L. Biferale, K. Binder, D. Dimitrov, F. Diotallevi, A. Milchev, and S. Succi, *J. Stat. Mech.* (2009) P06007.
 [26] A. A. Saha and S. K. Mitra, *J. Colloid Interface Sci.* **339**, 461 (2009).
 [27] T. S. Jiang, S. G. Oh, and J. C. Slattery, *J. Colloid Interface Sci.* **69**, 74 (1979).